Heavy-ion partial beam lifetimes due to Coulomb induced processes

A. J. Baltz,[1] M. J. Rhoades-Brown,[2,*] and J. Weneser[1]
[1]*Physics Department, Brookhaven National Laboratory, Upton, New York 11973*
[2]*Relativistic Heavy-Ion Collider Project, Brookhaven National Laboratory, Upton, New York 11973*
(Received 29 April 1996)

The magnitude of heavy-ion beam loss at the relativistic heavy ion collider (RHIC) and the large hadron collider (LHC) due to Coulomb induced bound-electron–positron production and to Coulomb dissociation of the nucleus is evaluated. With the nominal design parameters, the associated partial beam lifetime of RHIC (assuming four intersection regions) is calculated as 7.7 h and that of LHC (one intersection region) as 5.3 h. [S1063-651X(96)09510-4]

PACS number(s): 29.27.−a, 25.75.−q, 34.90.+q

I. INTRODUCTION

In ultrarelativistic heavy-ion colliders such as the relativistic heavy ion collider (RHIC) and the large hadron collider (LHC) there are two Coulomb induced processes occurring during beam crossing that provide stringent limits on the beam lifetime: bound-electron–positron pair production and dissociation of the nucleus. Both of these processes occur for ion trajectories of large enough impact parameter that there is no nuclear overlap of the colliding ions. In both processes each ion may be viewed in its own rest frame as being acted on by the Lorentz transformed Coulomb field generated by the other ion. In the first process an electron is produced in a bound state of the ion, thereby changing the charge of the ion and causing it to fall out of the beam. In the second process the Coulomb force dissociates the nucleus itself and the fragments fall out of the beam. Each of these processes has a cross section many times the geometric cross section for the collisions of Au + Au at RHIC or Pb + Pb at LHC, and it therefore turns out that these two Coulomb processes provide the primary limitation on beam lifetime. Continuum pair-production, in spite of its large cross section, does not cause beam deterioration, since (i) the average energy-momentum loss is only a minor fraction of the bunch dispersion and (ii) the r.f. acts to maintain the bunch.

In this paper we present comparative calculations of partial beam lifetimes due to Coulomb induced processes for the designed 100 GeV × 100 GeV Au + Au collisions at RHIC and 2.76 TeV × 2.76 TeV Pb + Pb collisions at LHC. In Sec. II we briefly review the results of our previous calculations of bound-electron–positron pair cross sections as applied to RHIC and LHC. In Sec. III we present the main calculations of this work: an evaluation of the Coulomb dissociation cross sections at RHIC and LHC based on an ''equivalent photon'' picture of the interaction combined with experimentally determined nuclear photoelectric cross sections that have been reported in the literature by various groups over many years. In Sec. IV we discuss formulas for the beam lifetimes, gather the design parameters, and calculate the partial beam lifetimes. In Appendix A we discuss in some detail the justification of ignoring higher order terms that are appreciable at small impact parameters in our Coulomb dissociation calculations of Sec. III. Appendix B reviews the damping mechanism that enters importantly at small impact parameters where the interaction is strong enough to invalidate a perturbational treatment. By summing a subset of terms, a prescription for dealing with the damping problem follows, and is used in Sec. III to make the small but necessary correction.

II. BOUND-ELECTRON–POSITRON PAIR PRODUCTION

We have shown [1] that in the ultrarelativistic limit the total perturbative cross section in Pb + Pb reactions for producing a positron and an electron in an orbit about one of the ions is given by the expression

$$\sigma_{\rm pert} = 14.3 \ln\gamma - 31 \text{ barns}, \tag{1}$$

where γ is the effective relativistic γ of one ion seen in the rest frame of the other ion. γ is 2.3×10^4 for RHIC and 1.7×10^7 for LHC. Since the perturbative treatment is invalid at small impact parameters a full coupled channel calculation was carried out to smoothly connect with the perturbative at larger impact parameters. The nonperturbative enhancement for relatively small impact parameters adds an energy-independent contribution of only about 7 barns to the previous expression and we have

$$\sigma_{\rm pair} = 14.3 \ln\gamma - 24 \text{ barns} \tag{2}$$

for Pb + Pb. To obtain cross sections for other colliding ions one recalls that the charge dependence goes approximately as $Z^{6.7}$, at least for ion pairs that range from iodine to uranium. The *K*-electron–positron cross section is calculated to be 93 $\pm\sim$ 5% barns for Au + Au at RHIC and 214 $\pm\sim$ 5% barns for Pb + Pb at LHC. Finally, the production of non-*K*-electron positron pairs is estimated to add approximately another 25% ± 5% to the cross section, giving us 117 ± 7% barns for RHIC and 268 ± 7% barns for LHC.

III. COULOMB DISSOCIATION

The cross section for heavy-ion dissociation is approximated (to within higher orders in $1/\gamma$) by the usual Weizsacker-Williams expression (for a review see Bertulani and Baur [2])

*Present address: Renaissance Tech Corporation, 25 East Loop Road, Stony Brook, NY 11790.

$$\sigma_{\rm dis}=\frac{2\alpha Z_p^2}{\pi\gamma^2}\int_{\omega_{\rm thresh}}^{\infty}d\omega\,\omega\sigma_{\rm ph}(\omega)\int_{b_0}^{\infty}bdbK_1^2\left(\frac{b\omega}{\gamma}\right). \quad (3)$$

$\sigma_{\rm ph}(\omega)$ is the photon cross section and is weighted by the energy dependent impact parameter integral over the square of the Bessel function. The approach, data sources, and methodology are much as in an earlier report [3] covering Coulomb dissociation at RHIC. The impact parameter range is restricted to values above the grazing value, b_0, thereby making a cut to eliminate the strong force nuclear interactions, which are counted separately. The b_0 is taken to be at just over twice the nuclear radius; since the b_0 dependence is weak we take it to be 15 fm for both Au and Pb. Appendix A provides some detailed discussion of corrections to the Weizsacker-Williams formulation that depend on the structure of the target nucleus, and, in particular, shows the smallness of the higher order terms not included in Eq. (3). There is implicit in Eq. (3) also an assumption that the probability of an ion dissociating is significantly less than unity for all impact parameters that contribute since it is an approximate perturbative form. But, as we will see later, our calculated first order probabilities go to unity near the grazing impact parameter. Therefore, we will use an appropriately modified expression for the cross section in the actual calculations described below. However, it is instructive to begin by analyzing the ω and b dependence of the cross section in terms of the approximately correct Eq. (3).

The impact parameter integral that appears in Eq. (3) may be carried out analytically,

$$\int_{b_0}^{\infty}bdbK_1^2\left(\frac{b\omega}{\gamma}\right)=(b_0^2/2)\left[K_0\left(\frac{b_0\omega}{\gamma}\right)K_2\left(\frac{b_0\omega}{\gamma}\right)-K_1^2\left(\frac{b_0\omega}{\gamma}\right)\right], \quad (4)$$

and the right-hand side may then be approximated very accurately for $b_0\omega/\gamma<1$ to yield

$$\int_{b_0}^{\infty}bdbK_1^2\left(\frac{b\omega}{\gamma}\right)=\frac{\gamma^2}{\omega^2}\left[\ln\left(\frac{2\gamma}{b_0\omega}\right)-\gamma_{\rm Euler}-0.5\right]=\frac{\gamma^2}{\omega^2}\ln\left(\frac{0.681\gamma}{b_0\omega}\right). \quad (5)$$

Putting in the factor of $\hbar c$ explicitly we obtain the familiar form

$$\sigma_{\rm dis}=\frac{2\alpha Z_p^2}{\pi}\int\frac{d\omega}{\omega}\sigma_{\rm ph}(\omega)\ln\left(\frac{0.681\hbar c\gamma}{b_0\omega}\right). \quad (6)$$

The lower limit of the ω integration is the neutron separation energy ($\omega_{\rm thresh}=8.1$ MeV for Au; 7.4 MeV for Pb). The situation at the high energy end of the integral is clear and straightforward. The approximate Eq. (5) neglects terms in $(b_0\omega/\hbar c\gamma)^2$. For ω large enough that the difference between the two expressions is non-negligible (where the argument of the logarithm approaches unity), the contribution to the integral is relatively insignificant. At that point the exact expression, Eq. (4), has become very small and is falling exponentially with ω: it effectively cuts off at $\omega=0.681\hbar c\gamma/b_0$. There is no difficulty with use of the exact form where necessary, but the approximation is very useful at low ω.

To address the unitarity problem, we recall that the fundamental formulation is in terms of a probability $P(b)$ which is summed over impact parameters and energy to give the total cross section,

$$\sigma_{\rm dis}=2\pi\int_{b_0}^{\infty}P(b)bdb. \quad (7)$$

The first order probability of dissociation $P_1(b)$ (the subscript is added here to emphasize the perturbational aspects) is that given by the Weizsacker-Williams approximation,

$$P_1(b)=\frac{\alpha Z_p^2}{\pi^2\gamma^2}\int d\omega\,\omega\sigma_{\rm ph}(\omega)K_1^2\left(\frac{b\omega}{\gamma}\right), \quad (8)$$

where $\sigma_{\rm ph}$ is understood to be the usual one-photon function. For $b\omega/\gamma\ll1$, $K_1^2\simeq(\gamma/b\omega)^2$, and the $1/b^2$ dependence makes the interaction large at small b; further the magnitude is increased for small b by $\sigma_{\rm ph}$ contributing up to very large values of ω before exponential cutoff by K_1 at $b\omega/\gamma\sim1$; at the largest values of b only the lowest energy part of $\sigma_{\rm ph}$ contributes.

Appendix B reviews the arguments for the introduction of the damping required to insure unitarity by the simple and plausible expression

$$P(b)\rightarrow1-\exp(-P_1(b)). \quad (9)$$

In the calculations we report on below, Eq. (9) was utilized, and the $\sigma_{\rm dis}$, Eq. (7), evaluated numerically.

The values for $\sigma_{\rm ph}(\omega)$ were taken directly from experiment wherever possible, and interpolated as needed. In the region of the giant dipole resonance, measurements were made for both Au and Pb targets by Veyssière [4] *et al.* from the neutron separation threshold (8.1 MeV for Au; 7.4 MeV for Pb) up to 25 MeV and the data fitted to Lorentz shapes, and we have used these fits for $\sigma_{\rm ph}(\omega)$ in this region. For the range 25 MeV $\leqslant\omega\leqslant$ 103 MeV, the work of Leprêtre [5] *et al.* was used. These data are for ^{208}Pb and $\sigma_{\rm ph}$ was scaled as 197/208 to obtain the Au values. For the range 103 MeV $\leqslant\omega\leqslant$ 440 MeV the Pb data of Carlos [6] *et al.* were used and again scaled for the Au calculations. For ω values in the range 440 MeV $\leqslant\omega\leqslant$ 2 GeV there are no experimental measurements of $\sigma_{\rm ph}$ for Au or Pb, and so we used scaled values of the (γ,p) [7] and (γ,n) [8] experimental cross sections of Armstrong *et al.*, i.e., $\sigma_{\rm ph}(\omega)=Z_T\sigma_{\gamma,p}(\omega)+(A_T-Z_T)\sigma_{\gamma,n}(\omega)$ ($T=$ target). For the range 2 GeV $\leqslant\omega\leqslant$ 16.4 GeV the Au data of Michalowski [9] *et al.* and Pb data of Caldwell [10] *et al.* were interleaved with suitable Z scaling.

In the region above 16.4 GeV there are no systematic $\sigma_{\rm ph}$ data for heavy targets, and above 17.84 GeV no (γ,n) data. We therefore must use (γ,p) data scaled by an effective number of nucleons. The data of Michalowski [9] and the data of Caldwell [10] indicate that for ω values greater than 17.84 GeV it is necessary to multiply $A_T\sigma_{\gamma,p}$ by a shadowing factor to take into account the fact that not all nucleons contribute to the photonuclear cross section. Based on

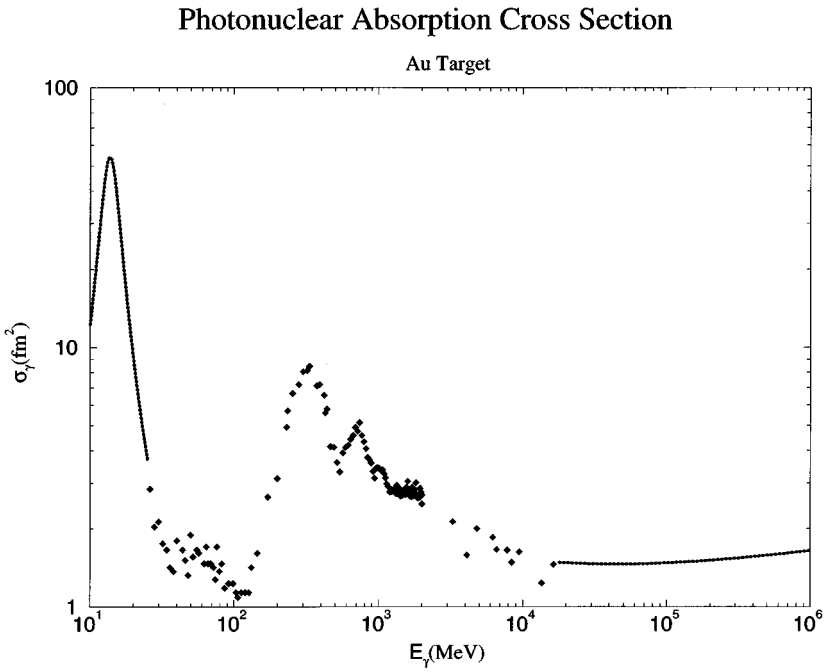

FIG. 1. Photonuclear absorption cross section taken from the work of Refs. [3–14] as utilized for these Au + Au Coulomb dissociation calculations.

the data at highest ω of these two data sets we take the shadowing factor to be 0.65, a value consistent with the experimental shadowing factor for Pb at 60 GeV [11]. For $\omega \geqslant 18$ GeV the (γ,p) cross sections are smooth and flat with only a gentle rise with increasing ω. The data have been very successfully described by a Regge theory parametrization [12]. More recent cross-section measurements in the region $\omega = 20\,000$ GeV [13–15] are also consistent with the Regge parametrization. Therefore above $\omega = 16.4$ GeV we make use of the Regge parametrization formula scaled by the shadowing factor (0.65) times the number of nucleons. Figure 1 summarizes this experimental input to our calculations for the Au + Au case.

In Table I, results for the dissociation cross section are presented as a function of an upper limit of $\omega, \omega_{\max}$, to illustrate scaling between the two machines at lower energy and the relative weighting of the very high energy equivalent photons (of which we know the least). At lower values of $\omega_{\max}$ the scaling between RHIC and LHC is approximately described by Eq. (6): $\sigma_{\rm dis}$ scales roughly as $[(82/79)^2(208/197)\ln\gamma]$, 1.9. Due to the much higher effective γ of LHC there are significant but minor contributions, $\sim 10\%$, to the integral Eq. (6) from values of ω above 18 GeV.

The total dissociation cross section of 220 barns for Pb + Pb at LHC is more than twice the 95 barns of Au + Au at RHIC. At RHIC energies the dissociation cross section for Pb + Pb is calculated as 110 barns.

The difference between $P(b)$ of Eq. (9) and $P_1(b)$ is significant near grazing impact parameters, as is illustrated in Fig. 2. In fact $P_1(b)$ is greater than unity for b less than 14.5 fm at RHIC and for b less than 17.5 fm at LHC; the lower limit $b_0 = 15$ fm means inclusion of some of the parameter range which requires damping. However, by far the largest part of the cross section builds up from impact parameters large enough that there is no significant difference between $P(b)$ and $P_1(b)$: the $1/b$ falloff in the cross-section integral does not completely cut off until about 10^{-7} cm at RHIC or until about 1 μm at LHC. To judge sensitivity to our various assumptions, note the following: use of the first order expression Eq. (8) rather than Eq. (9) leads to a cross section only 3 barns higher for Au + Au at RHIC and 6 barns higher for Pb + Pb at LHC. Setting b_0 equal to 17 fm rather than the 15 fm of these calculations only reduces the cross section by about 1 barn for RHIC and by 3 barns for LHC.

Given the extrapolations made necessary by the absence of applicable data, a completely reliable error estimate is made difficult. However, since the lower energies are heavily weighted, we can rely on the experimental errors for the photonuclear cross sections and assign a 5% error. To this

TABLE I. Dissociation cross section $\sigma_{\rm dis}$ (in barns) at RHIC and LHC.

$\omega_{\max}$ (MeV)	$\sigma_{\rm dis}(\omega_{\max})$ (Au + Au at RHIC)	$\sigma_{\rm dis}(\omega_{\max})$ (Pb + Pb at LHC)	Ratios
25	65	127	2.0
103	70	139	2.0
440	82	166	2.0
2000	90	187	2.1
17840	94	200	2.1
∞	95	220	2.3

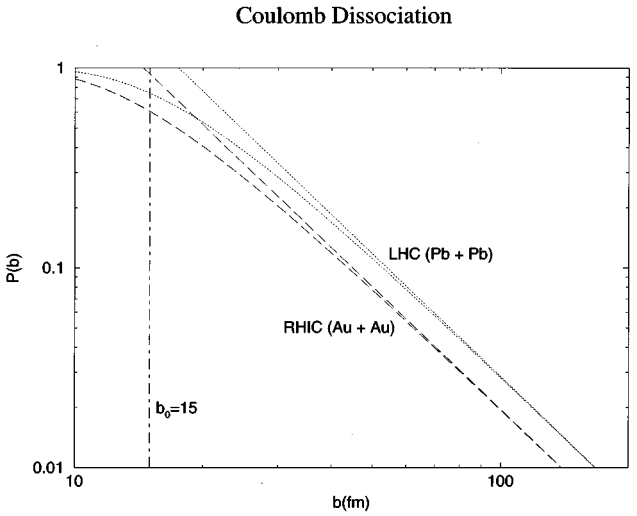

FIG. 2. Probability of Coulomb dissociation as a function of impact parameter. The dashed lines are for RHIC, dotted for LHC. The curves that turn over at small b are $P(b)$, the ones that go to unity are $P_1(b)$ (see text).

we add a 2% error from the high energy regions, leaving us with a quadratically combined 5.5% error to the overall cross sections. We have then $\sigma_{\rm dis}=95\pm5$b for RHIC, and 220 ± 12b for LHC. We note the agreement with the evaluation of Vidović, Greiner, and Soff [16].

IV. BEAM LIFETIMES

In Table II we gather together the ingredients for the computation of the partial beam lifetimes due to the Coulomb processes [17,18]. The equation for the partial beam loss may be written

$$\frac{d\eta}{dt}=-N_I\mathcal{L}\sigma_c, \tag{10}$$

where N_I is the number of intersection regions in the collider, η is the number of ions in the beam, $\mathcal{L}$ is the instantaneous luminosity, and σ_c is the sum of the Coulomb cross sections $\sigma_{\rm dis}$ and $\sigma_{\rm pair}$. $\sigma_c=212\pm10b$ (RHIC), $488\ \pm22b$ (LHC). Since the luminosity is proportional to the product of the ions in each beam or η^2, the solution to Eq. (8) may be written

$$\eta=\frac{\eta_0}{1+\frac{1}{2}\lambda t}, \tag{11}$$

where

$$\lambda=-2\left(\frac{d\eta}{dt}\right)_0\Big/\eta_0=-\left(\frac{d\mathcal{L}}{dt}\right)_0\Big/\mathcal{L}_0 \tag{12}$$

in terms of the initial values of η, $\mathcal{L}$ and their first derivatives. From Eq. (10) we also have

$$\lambda=2\frac{N_I\mathcal{L}_0\sigma_c}{\eta_0}. \tag{13}$$

The time development of the luminosity is then

$$\mathcal{L}=\frac{\mathcal{L}_0}{\left(1+\frac{1}{2}\lambda t\right)^2}. \tag{14}$$

Since at moderately short times, $\lambda t\ll1$,

$$\frac{1}{\left(1+\frac{1}{2}\lambda t\right)^2}\simeq e^{-\lambda t}, \tag{15}$$

it has become conventional to define a half-life in terms of λ as if there were exponential decay:

$$T_{\mathcal{L}_0}^{1/2}=\frac{\ln 2}{\lambda}. \tag{16}$$

Note, however, that the drop-off described by Eqs. (11) and (14) is slower than exponential. Note also that the half-life of the beam (η) is twice that of the luminosity ($\mathcal{L}$).

For the stated parameters, the partial half-lives due to Coulomb interactions are 45% longer for RHIC (7.7 ± 0.4 h) than for LHC (5.3 ± 0.2 h). Although the luminosity for LHC is twice that of RHIC, the four intersections of RHIC versus one for LHC give RHIC twice as many (hadronic) interactions per unit time. Note also that we are comparing initial luminosities; average luminosities would be somewhat smaller for both machines.

TABLE II. Beam lifetimes at RHIC and LHC. (Data from Refs. [15] and [16].)

	RHIC	LHC
Energy	100 GeV × 100 GeV	2.76 TeV × 2.76 TeV
Beam	Au + Au	Pb + Pb
$\gamma_{\rm eff}$	2.3×10^4	1.7×10^7
Luminosity $\mathcal{L}_0$	$0.84\times10^{27}/\mathrm{cm}^2$ sec	$1.95\times10^{27}/\mathrm{cm}^2$ sec
Number of ions η_0	5.7×10^{10}	5.2×10^{10}
Intersections N_I	4	1
$\sigma_{\rm dis}$	95 barns	220 barns
$\sigma_{\rm pair}$	117 barns	268 barns
λ	0.09/h	0.13/h
$T_{\mathcal{L}_0}^{1/2}$	7.7 h	5.3 h

ACKNOWLEDGMENTS

We acknowledge useful discussions about collider performances with P. D. Bond and M. A. Harrison, and about photonuclear cross sections with A. Nathan and A. Sandorfi. This manuscript has been authored under Contract No. DE-AC02-76-CH00016 with the U.S. Department of Energy.

APPENDIX A: THE WINTHER-ALDER CORRECTION TERMS

The Weizsacker-Williams formalism follows from a number of simplifying approximations: (i) unperturbed straight line trajectories of the heavy ions; (ii) very high ion energies that validate the expansion in powers of $1/\gamma$ and the discard of all but the leading terms; (iii) neglect of the internal transverse dimensions, ρ, of the excited target system relative to that of the projectile's impact parameter, b. It is this last assumption that is not valid for impact parameters of the order of the target system dimensions, and the Winther-Alder formalism [19] takes that into account via a full multipole expansion of the interaction.

Their results can also be obtained by expansion in powers of ρ/b of the perturbative transition amplitude, so that the connection with the usual Weizsacker-Williams form is immediately apparent. In the limit of large γ, the perturbative transition amplitude is given by

$$a_{of}(b) = 2\alpha Z_p \int d\tau \psi_f^* \frac{\vec{j}\cdot(\vec{b}-\vec{\rho})}{|\vec{b}-\vec{\rho}|}\psi_0 e^{i\omega z}\left\{\frac{1}{\gamma}K_1\left(\left|\frac{\vec{b}-\vec{\rho}}{\gamma}\right|\omega\right)\right\}; \tag{A1}$$

here all quantities and functions are evaluated in the rest system of the target, so that nonrelativistic nuclear physics applies; $\vec{j}$ is the electromagnetic current; $\vec{b}$ is the impact vector that lies in the $x-y$ plane orthogonal to the ion trajectories $\hat{z}$; ω the wave-number $(E_f-E_0)/\hbar c$. K_1 is the modified Bessel function, whose asymptotic behavior is

$$K_1(x) = \begin{cases} \dfrac{1}{x}+O(x), & x \ll 1 \\ \left(\dfrac{\pi}{2x}\right)^{1/2} e^{-x}, & x \gg 1. \end{cases} \tag{A2}$$

The Weizsacker-Williams result follows immediately on going to the very large γ limit for K_1 and dropping powers of ρ/b:

$$a_{of}^{(0)}(b) = 2\alpha Z_p \int \psi_f^* \vec{j}\cdot\hat{b} e^{i\omega z}\psi_0\left[\frac{1}{\gamma}K_1\left(\frac{\omega b}{\gamma}\right)\right]d\tau \cong \frac{2\alpha Z_p}{\omega b}\int \psi_f^* \vec{j}\cdot\hat{b} e^{i\omega z}\psi_0 d\tau. \tag{A3}$$

The matrix element is recognized as that of a photon process except that the transverse polarization vector, $\hat{e}$, is replaced by the transverse impact vector $\hat{b}=\vec{b}/b$. As in photon processes the matrix element can be separated into a sum of different multipoles. In the long-wavelength limit, which is particularly useful here, the leading terms of the multipole expansion follow from expansion of the retardation factor,

$$\int \psi_f^* \vec{j}\cdot\hat{b} e^{i\omega z}\psi_0 d\tau = \int \psi_f^* \vec{j}\cdot\hat{b}(1+i\omega z\cdots)\psi_0 d\tau, \tag{A4}$$

thus

$$\int \psi_f^* \vec{j}\cdot\hat{b}\psi_0 d\tau = a_{E1} \tag{A5}$$

and

$$i\omega\int \psi_f^* \vec{j}\cdot\hat{b} z\psi_0 d\tau = \frac{i\omega}{2}\int \psi_f^*(\vec{j}\times\vec{r})\cdot(\vec{b}\times\hat{z})\psi_0 d\tau + \frac{i\omega}{2}\int \psi_f^*[(\vec{j}\cdot\hat{b})(\vec{r}\cdot\hat{z}) + (\vec{j}\cdot\hat{z})(\vec{r}\cdot\hat{b})]\psi_0 d\tau, \tag{A6}$$

$$= a_{M1}+a_{E2}. \tag{A7}$$

The electric quadrupole, a_{E2}, contribution is most easily recognized in terms of the simple decomposition (take $\hat{b}$ as the x axis),

$$\left[\frac{j_x z + j_z x}{2}\right] = -\frac{1}{2}[\vec{j}\otimes\vec{r}]_{J=2,\mu=+1}+\frac{1}{2}[\vec{j}\otimes\vec{r}]_{J=2,\mu=-1}. \tag{A8}$$

The $\otimes$ symbol denotes the tensor combination defined by the subscripts. We will not need higher order multipoles here.

The first order in ρ/b adds to $a_{of}^{(0)}(b)$,

$$a_{of}^{(1)}(b) = \frac{2\alpha Z_p}{\omega b}\int \psi_f^*\left[\frac{-j\cdot\vec{\rho}\,\omega}{\omega b}+\frac{2(\vec{j}\cdot\hat{b})(\vec{\rho}\cdot\hat{b})\omega}{\omega b}\right]e^{i\omega z}\psi_0 d\tau, \cong \frac{2\alpha Z_p}{\omega b}\int \psi_f^*\left[\frac{-\vec{j}\cdot\vec{\rho}\,\omega}{\omega b}+\frac{2(\vec{j}\cdot\hat{b})(\vec{\rho}\cdot\hat{b})\omega}{\omega b}\right]\psi_0 d\tau. \tag{A9}$$

The operator in the bracket can be usefully rewritten as

$$\frac{1}{\omega b}\left[\frac{-(j_x+ij_y)}{\sqrt{2}}\frac{(x+iy)\omega}{\sqrt{2}}-\frac{(j_x-ij_y)}{\sqrt{2}}\frac{(x-iy)\omega}{\sqrt{2}}\right], \tag{A10}$$

and so is recognizable as a sum of $(\mu=+2)$ and $(\mu=-2)$ components; more to the final point, it is just

$$\frac{1}{\omega b}[\vec{j}\otimes\vec{r}]_{J=2,\mu=+2}-\frac{1}{\omega b}[\vec{j}\otimes\vec{r}]_{J=2,\mu=-2}. \tag{A11}$$

Therefore, these terms are weighted by $(2/\omega b)$, relative to the $\mu=\pm1$ terms of order $(\rho/b)^1$. Since the different multipoles and different μ components add incoherently, there is thus added to the familiar lowest order transition probability,

$$P^{(0)}(b)=\int \frac{1}{\pi^2}\alpha Z_p^2\omega\sigma_{\rm ph}(\omega)\left[\frac{1}{\gamma}K_1\left(\frac{b\omega}{\gamma}\right)\right]^2 d\omega$$
$$\cong\int \frac{1}{\pi^2}\alpha Z_p^2\frac{\sigma_{\rm ph}(\omega)}{\omega}\frac{1}{b^2}d\omega, \qquad \text{(A12)}$$

the next order

$$P^{(1)}(b)=\int \frac{1}{\pi^2}\alpha Z_p^2\omega\sigma_{{\rm ph},E2}(\omega)\frac{4}{(\omega b)^4}d\omega. \qquad \text{(A13)}$$

The quantity $\sigma_{{\rm ph},E2}$ is made up of the isoscalar plus the isovector electric quadrupole portion of the full photon spectrum.

As estimates of the electric quadrupole excitations that lie above nuclear separation energies we use the giant isoscalar and isovector electric quadrupolar resonances. In ^{208}Pb the isoscalar strength is believed to lie at about 11 MeV, below the giant $a_{\rm E1}$; the isovector strength is believed to be above the giant $a_{\rm E1}$ at about 20 MeV [20]. For our purposes here we assume that the strengths are given by the energy-weighted sum-rule:

$$\int \sigma_{E2}d\omega\sim\frac{(2\pi)^2}{40}\frac{\hbar^2}{2m}A(\omega R)^2, \qquad \text{(A14)}$$

for the isoscalar and isovector components. [The energy-weighted sum-rule for $a_{\rm E1}$ is $(2\pi)^2\alpha(\hbar^2/2m)(NZ/A)$.]

Since the Winther-Alder correction is appreciable for low energies, small ωR, it is most useful to compare the $P^{(1)}(b)$ correction with just the giant $a_{\rm E1}$ resonance contribution to $P^{(0)}(b)$. As an order of magnitude estimate then

$$P^{(1)}(b)/P^{(0)}_{E1}(b)\sim\int\frac{4\sigma_{E2}(\omega)}{\omega^3b^4}d\omega\Big/\int\frac{\sigma_{E1}(\omega)}{\omega}\frac{1}{b^2}d\omega$$
$$\sim\frac{1}{10}\frac{\omega_{E1}}{\omega_{E2}}\frac{R^2}{b^2}\frac{A^2}{NZ}. \qquad \text{(A15)}$$

At the minimum impact parameter $b=2R$, the ratio is $\frac{1}{40}(\omega_{E1}/\omega_{E2})(A^2/NZ)\sim0.14$ for the isoscalar $a_{\rm E2}$, and ~0.26 for the isovector. However, this overstates the overall importance; the ratio of the impact parameter integrated values, which determine the observable heavy ion cross-sections, is

$$\int_{2R}^{\infty}P^{(1)}(b)d^2b\Big/\int_{2R}^{\infty}P^{(0)}_{E1}(b)d^2b$$
$$\sim\frac{1}{80}\frac{\omega_{E1}}{\omega_{E2}}\Big/\ln\left(\frac{\gamma}{2R\omega_{E1}}\right). \qquad \text{(A16)}$$

For a $\gamma\sim2\times10^4$ the logarithm is ~10, so that the relative contribution is of order 0.2%; since the low energy $a_{\rm E1}$ contribution is of the order of half the total electromagnetic disintegration cross-section it is clear that we can ignore these contributions, overall of the order of 0.1%, and well below the precision needs.

APPENDIX B: DAMPING

Obviously the unitarity problem points up the inadequacy of the lowest order (in $Z\alpha$) perturbation theory, and demands the damping produced by higher orders. Fortunately the difficulty is present only over the small range of impact parameters from grazing at 15 fm to $\sim$ 50 fm. As we have seen in the numerical computations, this region contributes relatively little to the overall result: using the perturbative expression Eq. (8) rather than the unitarity corrected Eq. (9) results in 225 barns rather than 220 for LHC and 98 barns rather than 95 for RHIC. We are thereby able to proceed by a rough approximation to the full damping problem.

This approach to the damping problem has been introduced [21] into the problem of colliding heavy ions to deal with that occurring in calculation of multiple pair production by energetic heavy ions. The procedure is based on the independence of the different pairs created — independent of each other via any direct interaction and not coupled through any perturbation of the ion motion by the creation of the pairs. The latter assumption is justified by the very large momentum of the ions, γAM_p, compared to the pair momenta of order $m_ec^2\ln\gamma$. The neglect of interactions between pairs can be seen as the neglect of order α corrections relative to order $Z_{\rm ion}\alpha$. The results follow via a restricted summation of higher orders that consist of any number of pair creations and annihilations in all possible sequences. Each pair, real or virtual, is taken as independent, ignoring Pauli blocking or other interactions.

The effective Hamiltonian may be seen as describing independent modes that are each capable only of creation from and annihilation back to a ground state independent of the number, nature, or degree of excitation of other modes. The probability of creating N pairs may then be written in terms of the lowest order, $P_1(b)$,

$$N\text{-pair Prob}=[P_1(b)]^N\exp(-P_1(b))/N! \qquad \text{(B1)}$$

and the summed probability is just

$$1-\exp(-P_1(b)). \qquad \text{(B2)}$$

A like solution to multiple very low energy photon (boson) production in charged particle reactions is a textbook discussion [22]. Excitation of a harmonic oscillator by a linear perturbation [23] is also describable by a Poisson probability distribution, and a summed probability of the exponential form Eq. (B2). Translation of the procedure to nuclear excitations is clearly not immediate since the assumptions of independence of nuclear modes and independence of the base state upon which an excitation is built are not accurate. However, it can be a qualitatively useful method. The important nuclear modes are to be taken as consisting of the following.

(i) The giant multipoles, of which only the giant $a_{\rm E1}$ will be critical. The broad, phenomenologically known multipole is taken as a continuum distribution of sharp modes whose strengths are such as to describe the width and peak energy. The sharp modes are the analogs of the pairs or photons of the previous discussion. The experimental demonstration of

the Brink hypothesis, which asserts that all states equally support giant a_{E1} excitations, provides a conceptual base.

(ii) The individual nucleon modes, where a photon interacts principally with individual nucleons with only minor modification by the surrounding nuclear inhabitants.

Since the contributions from the lower energy excitations, 15–40 MeV, can be attributed to the first class, and the higher energy excitations to the second, a takeover of the formalism appears reasonable with the damping form of Eq. (9).

[1] A. J. Baltz, M. J. Rhoades-Brown, and J. Weneser, Phys. Rev. A **44**, 5568 (1991); **47**, 3444 (1993); **48**, 2002 (1993); **50**, 4842 (1994).
[2] C. A. Bertulani and G. Baur, Phys. Rep. **163**, 299 (1988).
[3] M. J. Rhoades-Brown and J. Weneser, Brookhaven National Lab. Report No. BNL-47806, AD/RHIC-110 (July 1992).
[4] A. Veyssière, H. Beil, R. Bergère, P. Carlos, and A. Leprêtre, Nucl. Phys. **A159**, 561 (1970).
[5] A. Leprêtre, H. Beil, R. Bergère, P. Carlos, J. Fagot, A. de Miniac, and A. Veyssière, Nucl. Phys. **A367**, 237 (1981).
[6] P. Carlos, H. Beil, R. Bergère, J. Fagot, A. Leprêtre, A. de Miniac, and A. Veyssière, Nucl. Phys. **A431**, 573 (1984).
[7] T. A. Armstrong *et al.*, Phys. Rev. D **5**, 1640 (1972).
[8] T. A. Armstrong *et al.*, Nucl. Phys. **B41**, 445 (1972).
[9] S. Michalowski, D. Andrews, J. Eickmeyer, T. Gentile, N. Mistry, R. Talman, and K. Ueno, Phys. Rev. Lett. **39**, 737 (1977).
[10] D. O. Caldwell, V. B. Elings, W. P. Hesse, R. J. Morrison, and F. V. Murphy, Phys. Rev. D **7**, 1362 (1973).
[11] D. O. Caldwell *et al.*, Phys. Rev. Lett. **42**, 553 (1979).
[12] A. Donnachie and P. V. Landshoff, Phys. Lett. B **296**, 227 (1992).
[13] M. Derrick *et al.*, Phys. Lett. B **293**, 465 (1992).
[14] T. Ahmed *et al.*, Phys. Lett. B **299**, 374 (1993).
[15] M. Derrick *et al.*, Z. Phys. C **63**, 391 (1994).
[16] Mario Vidović, Martin Greiner, and Gerhard Soff, Phys. Rev. C **48**, 2011 (1993).
[17] RHIC Design Manual, BNL-52195 (1989).
[18] LHC Conceptual Design, CERN/AC/95-05 (LHC) (1995).
[19] A. Winther and K. Alder, Nucl. Phys. **A319**, 518 (1979).
[20] D. S. Dale, R. M. Laszewski, and R. Alarcon, Phys. Rev. Lett. **68**, 3507 (1992).
[21] G. Baur, Phys. Rev. A **44**, 4767 (1991); M. J. Rhoades-Brown and J. Weneser, *ibid.* **44**, 330 (1991); Ch. Best, W. Greiner, and G. Soff, *ibid.* **46**, 261 (1992); J. Eichler and W. E. Meyerhoff, *Relativistic Atomic Collisions* (Academic Press, 1995), Sec. 10.4.2.
[22] V. B. Berestetskii, E. M. Lifshitz, and L. P. Pitaevski, *Relativistic Quantum Theory I* (Pergamon Press, 1994), Sec. 95.
[23] E. Merzbacher, *Quantum Mechanics*, 2nd ed. (Wiley, 1969), Sec. 15.9.